Potential of Contactless Support Structures for Improving the Part Quality of AlSi10Mg PBF-LB Parts

Steffen Kramer*[1,2], Kai Drechsel[1], Michael Jarwitz[2] https://orcid.org/0000-0002-6200-669X, Volker Schulze[1] https://orcid.org/0000-0003-2428-4127, Frederik Zanger[1] https://orcid.org/0000-0003-4500-3005

[1] wbk Institute of Production Science (KIT), Karlsruhe, Germany
[2] IFSW Institut fuer Strahlwerkzeuge (University of Stuttgart), Stuttgart, Germany

* Corresponding Author: steffen.kramer@partner.kit.edu, +49 721 608-44288

Abstract

Support structures are usually required to prevent thermally induced deformation of parts during the PBF-LB process, but also cause an increased effort for post-processing and an insufficient surface quality of the produced parts. An approach to overcome these limitations, suggested in the literature, is the use of contactless support structures (CSS), which should act as a heat sink to avoid thermally induced deformation. This approach was already successfully tested for electron beam melting (PBF-EB). Therefore, the aim of the present study is the experimental investigation of the application of CSS for the PBF-LB process. Different part and support geometries were built to investigate the potential of CSS to reduce thermally induced deformation during the PBF-LB process. Several use cases were covered, including increased overhang angles for thin features and maximized overhang thickness. The literature results for PBF-EB and Ti6Al4V could not be confirmed for PBF-LB using AlSi10Mg. The thermally induced deformation could not be reduced and the experimental results indicate that the use of CSS is accompanied by counterproductive process mechanisms.

Keywords: support structure, part quality, deformation, surface quality, AlSi10Mg, powder bed fusion

1 Introduction

The powder bed fusion process using a laser beam (PBF-LB) is a fast-developing additive manufacturing (AM) technology for producing near net shape metal parts and is increasingly used in industrial applications. This is mainly due to the enabled fabrication of parts with a high degree of functional integration or light weight parts with complex geometries, e.g. internal cooling channels or bionic structures. Besides these benefits there are also some drawbacks associated with the PBF-LB process, mainly the rough as-built surface, which often needs post processing. The occurrence of complex residual stresses in the part can lead to illicit deformations [1]. Overhanging part features are particularly prone to this due to the relatively low deformation resistance. During the build process these deformations can lead to collisions with the recoater blade/lip and consequently to a build job failure. Therefore, typically support structures are used to mechanically prevent deformation in the printing process by fixing the part and especially the overhanging part features to the substrate plate and therefore ensure geometric fidelity. The parts can be stress relieved via heat treatment before being removed from the substrate plate. Furthermore, support structures absorb the recoater force and prevent the parts from tearing off the substrate plate. Finally, support structures inhibit an overheating of the parts by conducting the process heat away from the process zone. [2]

But support structures also come along with certain disadvantages. They necessitate a time-consuming design process and after the production process they need to be manually removed which results in a rugged surface. Due to these drawbacks a lot of studies aim at reducing support structures or even eliminating them with a customized process strategy. These approaches, e.g. preheating, modified scan strategies or laser process parameters, all target the optimization of the heat flux and part temperature and are described below:

In [3] a preheating strategy was used to reduce the difference between solidification temperature and the temperature of the solid part around the melt pool and therefore reducing the temperature gradient substantially, which eliminated deformations. Often heating is conducted via substrate plate heating. Consequently, the preheating temperature and therefore the effectiveness diminishes over the part height. The study was carried out with AlSi10Mg. To achieve similar results with materials possessing a higher melting point, a considerable infrastructural and energetic effort is needed. Other studies, e.g. [4] have investigated the influence of scan strategies on the resulting residual stresses. The results showed, that residual stress could be reduced by using the chess strategy with an optimized square size to achieve a homogeneous heat influx. Residual stresses can also be influenced by laser process parameters as it is shown in [5]. Low laser power and low scan speed seem beneficial for the resulting residual stress. This results in lower melt

pool temperatures. But it is counterproductive to productivity and is accompanied by the need to locally adjust the laser parameters. In several studies topology optimization was used to design support structures to precisely increase heat flux out of overhanging part features and therefore stabilize the process [6]. In [7] a new approach to prevent deformation for parts produced by powder bed fusion using an electron beam (PBF-EB) was presented: contactless support structures (CSS). Solid objects are manufactured with a small gap underneath overhanging features to act as a targeted heat sink. Hence, the heat flux out of the built part is increased, which leads to a homogeneous temperature distribution, a lower melt pool temperature and lower temperature gradients. The experiments were conducted with Ti6Al4V and a preheating temperature of 730 °C. It was shown that it was possible to print horizontal and inclined overhangs without deformation by applying solid heat sinks below the overhang. The gap between the heat sink and the part was determined at 0.63 mm. [8] showed for PBF-LB and Ti6Al4V, that CSS were beneficial for the downskin surface quality, since the faster solidifying melt pool did not penetrate into the underlying powder bed. In [9] it was shown for Ti6Al4V that CSS could have a positive effect on part deformation in the PBF-LB process. Consequently, the scope of this study is to experimentally evaluate the potential of CSS in the PBF-LB process for different applications with AlSi10Mg and investigate the underlying process mechanisms.

2 Experimental procedure

Experiments were carried out to investigate the influence of CSS on overhang deformation and were compared to parts produced with no support structures and standard block support structures. The microstructure was evaluated to assess the effect on the cooling rate. Based on the specimen geometry used in [7], four different specimen geometries (Fig. 1) were designed:

- Geometry A: pillar (base area: 10x10 mm², height: 20 mm) with horizontal overhang, two different overhang thicknesses (1.5 mm [7], 0.75 mm) and two different support volumes for the solid structure below (50 % and 100 %)
- Geometry B: pillar (base area: 10x10 mm², height: 20 mm) with inclined overhang with different angles (10°, 20°, 30°, 45°,60°) and an overhang thickness of 0.75 mm
- Geometry C: pillar (base area: 10x10 mm², height: 20 mm) with inclined overhang (20°) and different overhang thicknesses (1 mm, 1.5 mm, 3 mm, 5 mm)
- Geometry D: two pillars (base area: 10x10 mm², height: 20 mm) connected at the top with a horizontal overhang (10x10 mm², thickness: 1.5 mm); 50 % and 100 % support volumes.

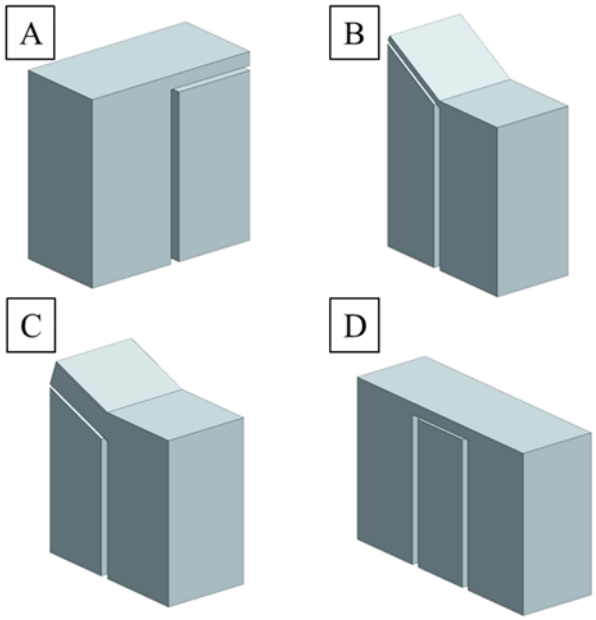

Figure 1: CAD models of the four used specimen geometries A-D

The gap between the pillar and the CSS was set to be 1 mm. Geometry A and D are designed to test horizontal overhangs whereby geometry A is the same geometry as in [7]. Geometry D is intended to bend only after it is cut from the substrate plate, to investigate the influence of CSS on the cooling rate and the emerging residual stress. Geometry B is designed to evaluate the influence of CSS on the minimum inclination angle possible to build, whereas geometry C is designed to test the maximum possible overhang thickness. As the average melt pool depth in solid material for the applied process parameters was measured at approx. 0.1 mm, the gap size between support and overhang for geometry A and D was varied from 0.1 mm to 0.25 mm with an increment of 0.05 mm. For the inclined geometries B and C larger gap sizes (B: 0.2 mm, 0.3 mm, 0.4 mm; C: 0.4 mm) were chosen, as heat accumulation was expected to occur in the gap due to the incline [8]. Every specimen was produced two times with a SLM280 HL by SLM Solutions. Process parameters were chosen to obtain high density parts (> 99,5%): laser power: 350 W, scan speed: 1050 mm/s, hatch distance: 170 µm, layer thickness: 50 µm. The laser beam focus diameter was 81 µm with a Rayleigh length of 3.57 mm and a wavelength of 1070 nm. The specimens were produced using the alternating chessboard scan strategy with a square size of 5x5 mm², as this strategy is proven to help reduce residual stresses [4]. Argon was used to create an inert process atmosphere. The substrate plate was preheated only to 100 °C to ensure that positive effects on the deformation could be attributed to the CSS and not the temperature of the substrate plate as in [3]. AlSi10Mg with a powder particle size distribution of - 20/+ 63 µm was chosen as specimen material, as it is widely used in PBF-LB and has a relatively high heat conduction coefficient, which should be beneficial for the

application. The specimens were cut from the substrate plate with wire electric discharge machining. The part deformation was measured with a tactile perthometer (Mahr PCV) on the up-bending upskin surface, as the specimen was fixed on one side. Three profiles were measured for each specimen (near the center and near the rim). As parameter for the deformation the angle between the horizontal and the balance line of the overhang profile was measured. Downskin quality was evaluated with a confocal microscope (Nanofocus Custom). Topography images were taken with a 10x objective (working distance: 12 mm), which resulted in a measurement field of 1,6 x 1,6 mm² and a lateral resolution of less than 1 µm. After aligning the topography and clearing it of any outliers, both Sa and Sz were calculated. For every specimen three statistically positioned topography images were taken. To assess the microstructure in geometry D, specimens were cold embedded, ground down by approx. 5 mm to reach the middle cross section, polished and etched with 2% NaOH etching agent. The microstructure was evaluated using a scanning electron microscope (SEM) (Jeol JSM-6010 LV) and measuring the dendritic arm spacing (DAS) at different points.

3 Results

3.1 Applicability for horizontal overhangs

For all specimens of geometry A & D with a gap size < 0.2 mm, the horizontal overhang was firmly fused to the CSS, see Fig. 2 a), and could not be removed manually without destroying the overhang. Consequently, they were exempted from further investigation. The specimens with an overhang thickness of 1.5 mm showed severe deformation for gap sizes of 0.2 mm and 0.25 mm and both support volumes during the build process. The deformation severely damaged the recoater lip, requiring the build process to be aborted. The build process for specimens with an overhang thickness of 0.75 mm was completed and the deformation was evaluated for gap sizes of 0.2 mm and 0.25 mm (Fig. 2). The recoater lip showed intensive scratch marks on the downside and had to be replaced. Because the overhang stayed attached to the support volume in some areas for a gap size > 0.2 mm due to powder sintering, the deviation of the deformation values is high, which is highlighted by the large error bars. For geometry D an overhang thickness of 1.5 mm was possible to build. As the overhang was fixed on both sides, deformation during the process was largely inhibited. Measurements of the angle between the balance line of the upskin profile and the horizontal indicate that neither the size of the support volume nor the gap size influence the resulting deformation (Fig 2). The deformation angle averages for every configuration between 1.5° and 1.75°. The deformation of the specimen built without support was only around 0.8° whereas the specimen built with conventional supports showed nearly no deformation.

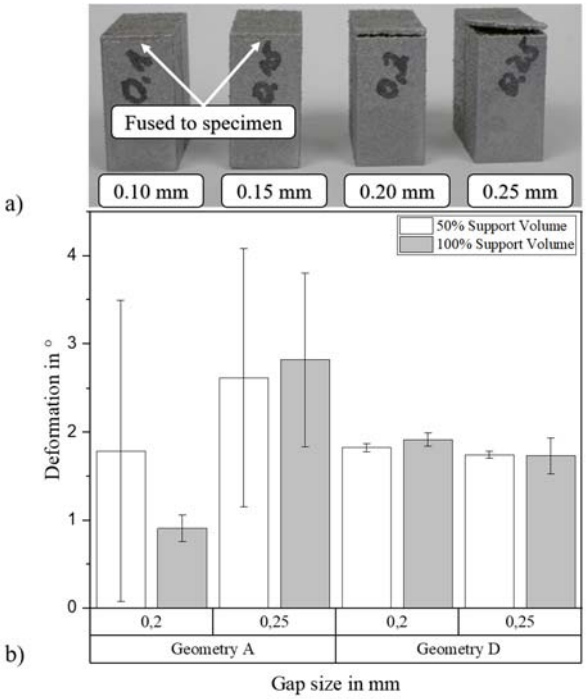

Figure 2: a) Specimens with horizontal overhangs (0.75 mm), full support volume and varying gap thickness, b) deformation angle for horizontal overhangs for varying support volumes and gap sizes. Error bar: standard deviation.

3.2 Applicability for inclined overhangs

All overhangs with a gap size of 0.2 mm were fixed to the CSS below whereas overhangs with a gap size of 0.3 mm were only fixed to the support volume for angles of 30° and smaller. However, there was no attachment for a gap size of 0.4 mm, which was therefore used for further evaluation. Measurement of the incline angle on the upskin shows that angles down to 20° are possible without considerable deformation for specimens with CSS and even specimens without any support structure. An inclination angle of 10° was feasible regardless of the use of CSS but resulted in a humped overhang shape, which indicates, that the process did not run stable. Specimens with 10° were therefore exempted from evaluation. Sa and Sz were evaluated on the downskin surface of specimens with a gap size of 0.4 mm and specimens without support volume to investigate the influence of CSS on the surface quality (Fig. 3). Especially for angles lower than 30° the downskin topography is dominated by sintered powder agglomerations and melt drops, which penetrated the underlying powder bed. Roughness values generally decrease with higher overhang angles but only for 30° and 45° both Sa and Sz are substantially lower with the use of a support volume. This could be due to a limited amount of powder in the gap, which can be absorbed by the propagating melt pool. The limited amount of available

powder and the solid surface of the CSS presumably hinder a further sinking of the melt pool into the powder bed which could explain the improved surface quality.

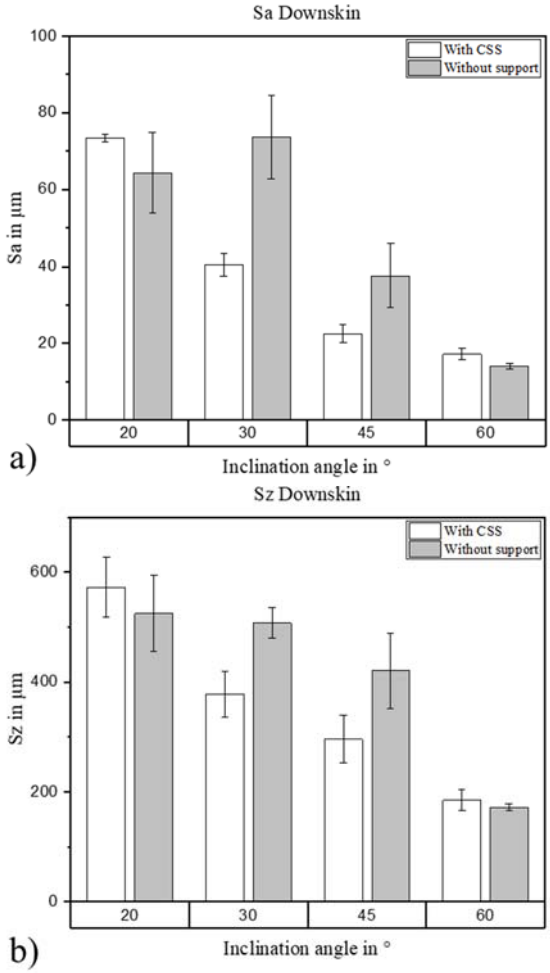

Figure 3: Geometry B: downskin surface roughness for different overhang angles and for specimens with and without CSS: a) Sa, b) Sz. Error bar: standard deviation.

The arising tensile stress in every processed layer, which causes the deformation, depends on the molten area in that layer [10]. Due to the part geometry, the maximum process area per part during the layerwise process is fairly small for an overhang thickness of 0.75 mm (merely larger than the upskin of the pillar) but grows with increased overhang thickness. Therefore, by enhancing the overhang thickness (geometry C) the potential of CSS to dissipate heat and therefore prevent deformation is tested. Regardless of the use of a support volume, specimens with an overhang thickness of 1.5 mm and more showed severe shape deformation. Although the upskin had good form accuracy the downskin bent up substantially as depicted in Fig 4. For an overhang thickness of 5 mm severe deformation during the process required the abortion of the printing process. An evaluation of the surface roughness showed, that the overhang thickness has no notable influence on the resulting downskin roughness (Fig. 5).

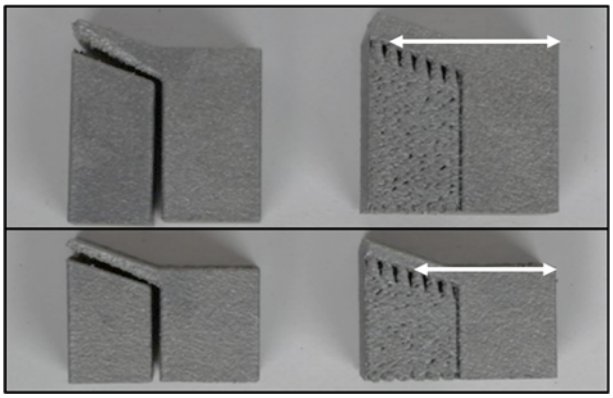

Figure 4: Geometry C: specimens with different target thickness: top: 3 mm, bottom: 1.5 mm. (left: with CSS, gap size: 0.4 mm; right: conventional block support) The white arrows indicate the layer with the maximum molten area.

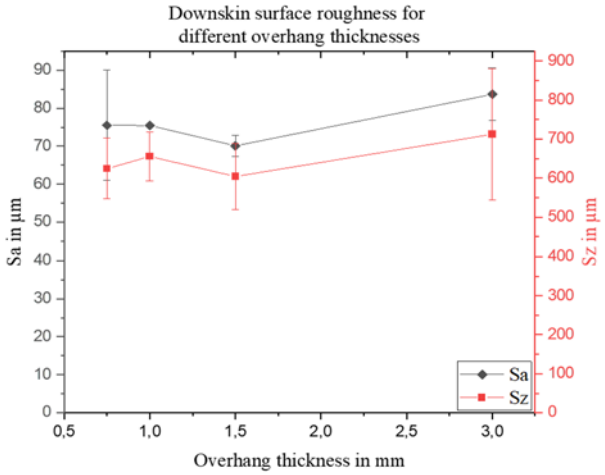

Figure 5: Geometry C: downskin surface roughness for different overhang thicknesses for specimens with CSS. Error bar: standard deviation.

3.3 Impact on heat dissipation

To further assess the impact of the CSS on the heat dissipation two geometry D specimens, (i) 0.25 mm gap size, full support volume; (ii) no support, were metallographically prepared and investigated with a scanning electron microscope.

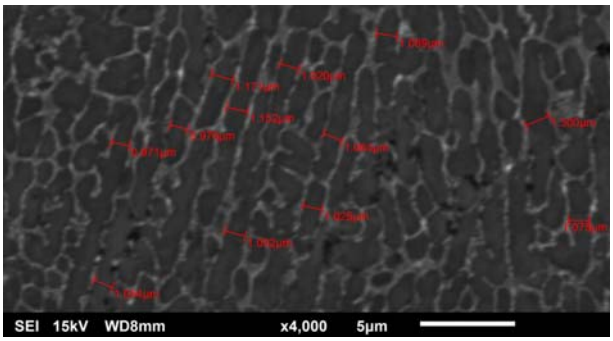

Figure 6: Geometry D: exemplary SEM picture with measurement of the DAS at several points in a columnar grain

Along the height of the overhang the DAS was measured and employed to calculate the cooling rate as presented in [11] (Fig 6). It is evident, that in the lower regions of the overhang the cooling rate is substantially higher for the specimen built with support volume (Table 1). From the middle regions of the overhang upwards, the difference is neglectable. Overall the cooling rate in the overhang is lower than in the solid pillar structure.

Table 1: DAS values and resulting cooling rate $\dot{T}$ at different points in the overhang for specimens with and without CSS. Average DAS values were calculated from a minimum of 20 measurement values with min. 3 different SEM images.

Table Nr. 1	With contactless support structure		Without support structure	
	DAS in µm	$\dot{T}$ in K/s	DAS in µm	$\dot{T}$ in K/s
Upskin	611	5.09E+05	550	7.05E+05
Middle	716	3.13E+05	671	3.83E+05
Downskin	724	3.03E+05	1132	7.62E+04
Solid Material	489	1.02E+06	477	1.10E+06

3.4 Simulation

A simulation of the occurring stresses and displacements to improve the explanation of the observed results, showed, that for thin overhangs the maximum stress is located in the upskin of the pillar and does not cause a deformation of the overhang. Consequently, thin overhangs are easy to build down to an angle of 20°. For thicker overhangs the maximum stress is located in the overhang. The consecutive simulation of the deformation also predicts the deformation of thicker overhangs as it was evident in geometry C (Fig. 7).

4 Discussion

For the specimens with an overhang thickness of 1.5-3 mm (geometry C) the moderate deformation of the tip of the overhang during the build process hinders the powder deposition. Therefore, no material gets added there and this area is repeatedly exposed to laser scanning and is presumably tempered, which inhibits further deformation. Meanwhile material is added in other areas, which gradually enhances the deformation resistance. Hence the deformation process stops and the build job can be finished. As a result, the overhang has a convex shape on the downside but is geometrically correct on the upper side. The results for geometry D predominantly confirm the results obtained for geometry A except the specimen without support, as one would expect the same or even higher deformation. Investigation of the microstructure indicates, that due to the isolating properties of the powder bed the cooling process was slowed down considerably without CSS.

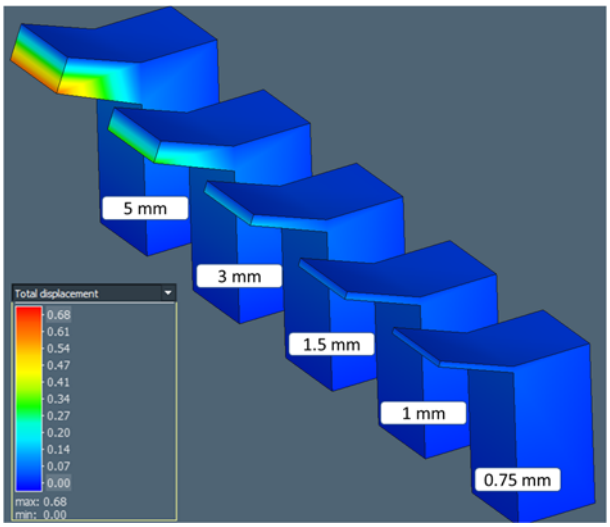

Figure 7: Geometry B: Simulation of the total displacement on the basis of inherent strains for different overhang thickness (0.75 mm – 5 mm). Simulation was carried out with Simufact Additive.

Summarizing, the results from PBF-EB with Ti6Al4V reported in literature (see [7,8]) could not be transferred to PBF-LB and AlSi10Mg. The approach of contactless support structures is based on fast, homogeneous heat dissipation. However, heat dissipation is not an instantaneous process, but requires time. This is particularly relevant for overhanging features considering that heat dissipation through the powder bed can be neglected, as the heat conduction coefficient of powder is 100-1000x lower as for solid material [10]. Besides the different material, other differences in the process possibly influence the heat dissipation. The results of geometry A indicate, that the melting and solidification process occur too fast. This seems plausible as the PBF-LB process has much higher cooling rates (10^5-10^7 K/s [11]) compared to PBF-EB (10^3-10^5 K/s [12]). This can be attributed to the higher melt pool temperature and the extremely local heat influx due to the smaller focus diameter of laser beams compared to electron beams. Also, the preheating temperature was - with respect to the materials melting point - lower for PBF-LB (0.43 T_S) compared to PBF-EB (0.52 T_S) in [8]. The results of this investigation necessitate the reconsideration of the contactless support structure mechanism. Following the temperature gradient model (TGM) and cooldown model [1], there are two options to reduce residual stresses in PBF-LB, which both aim at reducing arising compressive stresses in the solid material around the melt pool: a) Heat the surrounding solid material to reduce the temperature difference and enhance the elastic properties, which is the approach presented in [3]. b) Reduce the melt pool temperature in overhanging areas to assist heat dissipation either by adjusting the scanning parameters or by withdrawing

heat from the melt pool e.g. with CSS. The latter also leads to a higher heat dissipation in the surrounding material and in turn gives rise to compressive stress. The results in [7, 9] and the present study indicate that depending on the physical process conditions (cooling rate, melt pool temperature and material) either the melt pool temperature reduction or the cooling of the surrounding material dominate. The high cooling rate for PBF-LB suggests that melting and solidification occur too fast for efficient melt pool temperature reduction, which could be a possible explanation for the present results.

Further research for PBF-LB should be focused on the local adjustment of laser scanning parameters to adapt to the different heat dissipation in overhanging structures. The low heat conductivity of the underlying powder bed asks for lower energy densities. Also, the optimization process needs to be automated. Several software providers already offer this feature. Eventually the influence of the parameter adjustment on the part quality and part properties needs to be researched.

5 Conclusion

In the present work the concept of contactless support structures, known from publications concerning the PBF-EB process [7, 8], was experimentally evaluated to assess the potential for the application in the PBF-LB process. Four different geometries were manufactured with horizontal and inclined overhangs. Neither for horizontal overhangs nor for inclined overhangs a positive effect of CSS on the resulting deformation was observed. This is attributed to high cooling rates and a high melt pool temperature. However, CSS have a positive impact on the surface quality for inclined overhangs with angles of 30° to 45°. Microstructural investigations showed, that in the first few layers above the support volume the cooling rate is increased considerably. A theoretical analysis of the residual stress mechanisms during the process further indicates, that with CSS two counteractive mechanisms (lowering melt pool temperature vs. lowering temperature of surrounding material) limit the potential of CSS significantly. Therefore, further concepts to optimize the implementation or minimization of support structures should be aimed at locally adjusting the heat influx via laser scanning parameters.

Acknowledgements

The presented work was funded by the Ministry of Science, Research and the Arts of the Federal State of Baden-Wuerttemberg within the ‘InnovationCampus Future Mobility’, which is gratefully acknowledged.

Literature

[1] C. Li, Z.Y. Liu, X.Y. Fang and Y.B. Guo, “Residual stress in metal additive manufacturing”, Procedia CIRP 71, 2018, pp. 348-353

[2] M. Leary, T. Maconachie, A. Sarker, O. Faruque and M. Brandt, “Mechanical and thermal characterisation of AlSi10Mg SLM block support structures”, Materials and Design 183, 2019, 108138

[3] D. Buchbinder, W. Meiners, N. Pirch, K. Wissenbach and J. Schrage, „Investigation on reducing distortion by preheating during manufacturing of aluminium components using selective laser melting”, J. Laser Appl. 26, 2014, 012004

[4] J. Hajnys, M. Pagac, J. Mesicek, J. Petru and M. Krol, “Influence of scanning strategy parameters on residual stress in the SLM process according to the bridge curvature method for AISI 316L stainless steel”, Materials 13, 2020, 1659

[5] L. Wang, X. Jiang, Y. Zhu, X. Zhu, J. Sun and B. Yan, „An approach to predict the residual stress and distortion during the selective laser melting of AlSi10Mg parts”, Int J Adv Manuf Technol 97, 2018, pp. 3535-3546

[6] M. Leary, L. Merli, F. Torti, M. Mazur and M. Brandt, “Optimal topology for additive manufacture: a method for enabling additive manufacture of support-free optimal structures”, Materials and Design 63, 2014, pp. 678-690

[7] K. Cooper, P. Steele, B. Cheng and K. Chou, “Contact-free support structures for part overhangs in powder-bed metal additive manufacturing”, Inventions. 3(1), 2018, 2

[8] U. Paggi, R. Ranjan, L. Thijs, C. Ayas, M. Langelaar et al., “New support structures for reduced overheating on downfacing regions of direct metal printed parts”, Proceedings 30th Annual Solid Freeform Fabrication, 2019, pp. 1626-1640

[9] K. Zhang, G. Fu, P. Zhang, Z. Ma, Z. Mao et al., „Study on the geometric design of supports for overhanging structures fabricated by selective laser melting”, Materials 12, 2019, 27

[10] L. Parry, I.A. Ashcroft, R.D. Wildman, “Understanding the effect of laser scan strategy on residual stress in selective laser melting through thermo-mechanical simulation”, Additive Manufacturing 12, 2016, pp. 1-15

[11] H. Hyer, L. Zhou, A. Mehta, S. Park, T. Huynh et al., “Composition-dependent solidification cracking of aluminium-silicon alloys during laser powder bed fusion”, Acta Materialia 208, 2021, 116698

[12] H. Galarraga, R. Warren, D. Lados, R. Dehoff, M. Kirka, P. Nandwana, „Effects of heat treatments on microstructure and properties of Ti-6Al-4V ELI alloy fabricated by electron beam melting (EBM)”, Materials Science and Engineering: A 685, 2017, pp. 417-428